DEVELOPMENT OF A MATHEMATICAL MODEL FOR A SINGLE ALKALINE MEMBRANE FUEL CELL (AMFC) WITH FIXED VOLUME AND GENERAL SQUARE SECTION

Elise Meister Sommer[1], **elise.sommer@gmail.com**
Lauber de Souza Martins[2], **martins@caps.fsu.edu**
Juan Carlos Ordonez[2], **ordonez@eng.fsu.edu**
José Viriato Coelho Vargas[1], **jvargas@demec.ufpr.br**

[1] Universidade Federal do Paraná – UFPR. Bloco IV do Setor de Tecnologia, Centro Politécnico (Campus II), Bairro Jardim das Américas Cx. 19011, CEP 81531-990, Curitiba, PR Brasil

[2] Department of Mechanical Engineering and Center for Advanced Power Systems, Florida State University, Tallahasse, Florida 32310-6046, USA

Abstract. *The Alkaline Membrane Fuel Cell (AMFC) is a recently developed fuel cell type, which has shown good experimental results in the laboratory. This paper introduces a mathematical model for the single AMFC with fixed volume and general square section. The main objective is to produce a reliable model (and computationally fast) to predict the response of the single AMFC according to variations of the physical properties of manufacturing materials and operating and design parameters. The model is based on mass, momentum, energy and species conservation, and electrochemical principles, and takes into account pressure drops in the gas channels and temperature gradients with respect to space in the flow direction. The simulation results comprise the AMFC temperature distribution, net power and polarization curves. It is shown that temperature spatial gradients and gas channels pressure drops significantly affect fuel cell performance. Such effects are not usually investigated in the models available in the literature, with most of them assuming uniform pressure and temperature operation. Therefore, the model is expected to be a useful tool for AMFC design and optimization.*

Keywords: *Alkaline Membrane Fuel Cell; Mathematical Modeling; Pressure Drop*

1. INTRODUCTION

The Alkaline Membrane Fuel Cell (AMFC) is a recently developed fuel cell type, which has shown good experimental results in the laboratory. Alkaline Fuel Cells (AFC) are seen as an alternative for Polymer Electrolyte Membrane Fuel Cells (PEMFC) applications due the possibility of not using noble metals as catalyst, by allowing for example nickel to be the catalyst at the anode and silver at the cathode; which could be a good alternative when cost is considered an important issue. This paper studies an AMFC, in which the polymer electrolyte membrane used in PEMFC is replaced by a membrane made from cellulose and the used electrolyte is an alkaline solution, 30% KOH. This configuration still allows the fuel cell to work at low temperature, like PEMFCs do. With respect to the current AFC, the herein proposed AMFC has the advantage of a solid membrane made by cellulose instead of just a liquid electrolyte and does not require elaborated sealings to operate.

A mathematical model is introduced for the single AMFC with fixed volume and general square section. The main objective is to produce a reliable model (and computationally fast) to predict the response of the single AMFC according to variations of the physical properties of manufacturing materials and operating and design parameters.

2. MATHEMATICAL MODEL

A schematic diagram of the internal structure of a AMFC is shown in Fig. 1 and Fig. 2. Pure hydrogen and pure oxygen are considered in this analysis as fuel and oxidant respectively.

The approach chosen was to divide the fuel cell into seven control volumes that interact energetically with one another, with the ambient and with the adjacent fuel cell, in case of analysis of a stack. Two bipolar plates were added and they have the function of allowing the electrons produced by the electrochemical oxidation reaction at the anode to flow to the external circuit or to an adjacent cell.

The model consists of the conservation equations for each control volume, and equations accounting for electrochemical reactions, where they are present. The reversible electrical potential and power of the fuel cell are then computed as functions of the temperature and pressure fields determined by the model. The actual electrical potential and power of the fuel cell are obtained by subtracting from the reversible potential the losses due to surface overpotentials, slow diffusion and all internal ohmic losses through the cell. These are functions of the total cell current (I), which is directly related to the external load. In this model, the total current is considered an independent variable.

The control volumes (CV) are fuel channel (CV1), the anode diffusion-backing layer (CV2), the anode reaction layer (CV3), the alkaline membrane (CV4), the cathode reaction layer (CV5), the cathode diffusion backing layer (CV6) and the oxidant channel (CV7).

Dimensionless variables are defined based on the geometric and operating parameters of the system. Pressures and temperatures are referenced to ambient conditions: $P_i = p_i / p_\infty$ and $\theta_i = T_i / T_\infty$, where P is the dimensionless pressure, p is the pressure, N/m^2 ; θ is the dimensionless temperature, T is the temperature, K; the subscript i and ∞ represent the substance or a location in the fuel cell and the ambient respectively. Other dimensionless variables are defined as:

$$\psi = \frac{\dot{m}_i}{\dot{m}_{ref}} \tag{1}$$

$$N_i = \frac{U_{wi} V_T^{2/3}}{\dot{m}_{ref} c_{p,f}}, \quad \tilde{A}_i = \frac{A_i}{V_T^{2/3}} \tag{2}$$

where ψ and $\dot{m}$ are the dimensionless mass flow rate and mass flow rate kg/s, respectively; N is the dimensionless global wall heat transfer coefficient, U is the global wall heat transfer coefficient, W/m^{2}K; V_T is the total volume of the fuel cell, m^3; $c_{p,f}$ is the specific heat at constant pressure of the fuel, kJ/kgK; $\tilde{A}$ is the dimensionless area, A is the area, m^2; the subscript *i* indicates a substance or a location in the fuel cell, ref indicate the reference level and w indicates wall.

$$\xi_j = \frac{L_j}{V_T^{1/3}} \tag{3}$$

where L indicates the length, m; ξ is the dimensionless length ;the subscript j indicates a particular dimension of the fuel cell geometry, Fig. 2.

$$\tilde{h} = \frac{h V_T^{2/3}}{\dot{m}_{ref} c_{p,f}}, \qquad \tilde{k} = \frac{k V_T^{1/3}}{\dot{m}_{ref} c_{p,f}} \tag{4}$$

Where h is the heat transfer coefficient, W/m^{2}K; k is the thermal conductivity, W/mK; $\tilde{h}$ s the dimensionless heat transfer coefficient, $\tilde{k}$ is the dimensionless thermal conductivity.

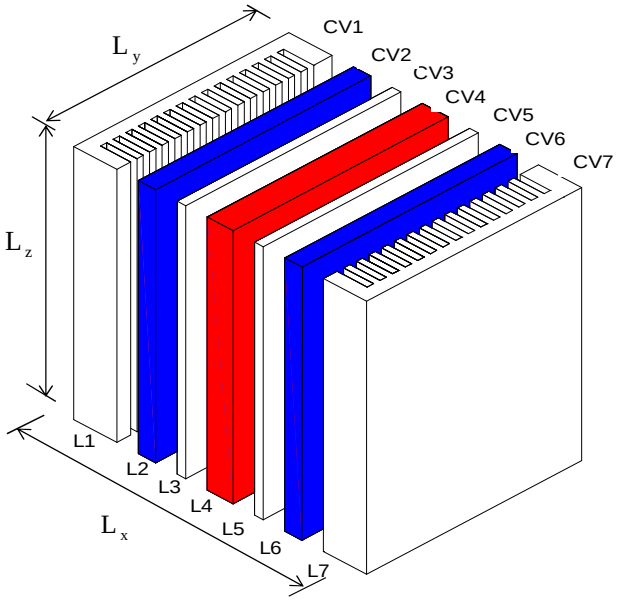

Figure 1. Single AMFC fuel cell model and control volumes distribution, L is the length of each CV, L_x is the total length of the fuel cell, L_z is the high and L_y is the width of the fuel cell.

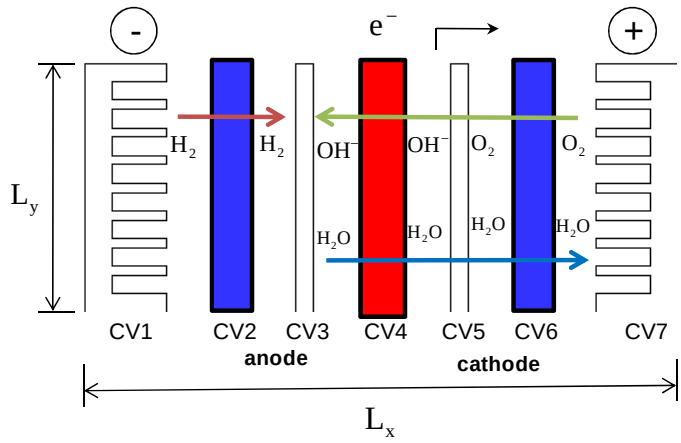

Figure 2. Upper view of the control volumes of a single AMFC fuel.

The hydrogen mass flow rate required for the current (I) dictated by the external load is

$$\dot{m}_{H_2} = \dot{n}_{H_2} M_{H_2} = \frac{I}{nF} M_{H_2} \tag{5}$$

Where ṅ is the molar flow rate, kmol/s; M is the molar weight,kg/kmol; n is the equivalent electron per mole of reagent, eq/mol; I is the total current, A; F is the Faraday constant, C/eq.

Therefore, the oxygen mass flow rate needed for a AMFC fuel cell is

$$\dot{m}_{O_2} = \frac{1}{2} \dot{n}_{H_2} M_{O_2} \tag{6}$$

2.1. Energy conservation

The wall heat transfer area of one control volume in the AMFC is $A_{wi} = \tilde{p}_s L_i \ \ (2 \le i \le 6)$ and $A_{wi} \cong \tilde{p}_s L_i + L_y L_z$ (i = 1,7;), where $\tilde{p}_s = 2(L_y + L_z)$ is the perimeter of the fuel cell cross-section. The control volumes are $V_j = L_y L_z L_j \ \ (2 \le j \le 6)$ and $V_j = n_c L_c L_l L_z$ (j =1, 7), where n_c is the integer part of $L_y/(L_t + L_c)$, i.e., the number of parallel ducts in each gas channel (fuel and oxidant). The mass and energy balances for CV1 yield the temperature in CV1,

$$\tilde{Q}_{w1} + \psi_f (\theta_f - \theta_1) + \tilde{Q}_{12} + \tilde{Q}_{1ohm} = 0 \tag{7}$$

and

$$\tilde{Q}_{wi} = N_i \tilde{A}_{wi} (1 - \theta_i), \ \tilde{Q}_{iohm} = I^2 \beta_i / \left(\dot{m}_{ref} c_{p,f} T_\infty \right) \tag{8}$$

where $\tilde{Q}_{12} = \tilde{h}_1 \tilde{A}_s (1 - \phi_2)(\theta_2 - \theta_1)$, $\tilde{A}_s = L_y L_z / V_T^{2/3}$. Subscript i represents a location in the cell, i.e., a particular CV, f indicates fuel, ohm indicates ohmic and ϕ the porosity. The dimensionless heat transfer rates for all the compartments are $\tilde{Q}_i = \dot{Q}_i / \dot{m}_{ref} c_{p,f} T_\infty$. The subscript i accounts for any of the heat transfer interactions that are present in the model. $\dot{Q}$ is the heat transfer rate, W; $\tilde{Q}$ is the dimensionless heat transfer rate, β is the electrical resistance, Ω.

Assuming that the channels are straight and sufficiently slender, and using the ideal gas model, the pressure drops are

$$\Delta P_i = n_c f_i \left(\frac{\xi_z}{\xi_i} + \frac{\xi_z}{\xi_c} \right) \frac{P_j}{\theta_i} \frac{R_f}{R_i} \tilde{u}_i^2 \tag{9}$$

where i = 1,7 and j = f (fuel), ox (oxidant), respectively. Here $\tilde{u}_i = (\tilde{u}_{i,in} + \tilde{u}_{i,out})/2$ is the channel dimensionless mean velocity, defined as $\tilde{u} = u/(R_f T_\infty)^{1/2}$, and f is the friction factor, ξ_c is the dimensionless width of the gas channels, R is the ideal gas constant kJ/kgK. According to mass conservation, the dimensionless mean velocities in the gas channels are

$$\tilde{u}_1 = \frac{C\theta_1}{\tilde{A}_{c1}P_f}\left[\psi_f - \frac{\psi_{H_2}}{2}\right] \tag{10}$$

$$\tilde{u}_7 = \frac{R_{ox}C\theta_7}{R_f\tilde{A}_{c7}P_{ox}}\left[\psi_{ox} - \frac{\psi_{O_2}}{2}\right] \tag{11}$$

$$C = \frac{(R_f T_\infty)^{1/2}\dot{m}_{ref}}{p_\infty V_T^{2/3}} \tag{12}$$

where $\tilde{A}_{ci} = n_c L_c L_i / V_T^{2/3}$, i = 1,7 and L_c is the width of the gas channel, m.

For the laminar regime, $\mathrm{Re}_{D_h} < 2300$ (Shah and London, 1978):

$$f_i \,\mathrm{Re}_{Dh,j} = 24(1 - 1.3553\delta_i + 1.9467\delta_i^2 - 1.7012\delta_i^3 + 0.9564\delta_i^4 - 0.25371\delta_i^5) \tag{13}$$

$$\frac{h_i D_{h,i}}{k_i} = 7.541(1 - 2.610\delta_i + 4.970\delta_i^2 - 5.119\delta_i^3 + 2.702\delta_i^4 - 0.548\delta_i^5) \tag{14}$$

where $\delta_i = L_c/L_i$, for $L_c \le L_i$ and $\delta_i = L_i/L_c$, for $L_c > L_i$; $D_{h,i} = 2L_c L_i/(L_t + L_c)$, $\mathrm{Re}_{Dh,i} = u_i D_{h,i}\rho_i/\mu_i$ and i = 1,7. According to Bejan (1995), the correlations used for the turbulent regime are

$$f_i = 0.079\mathrm{Re}_{Dh,i}^{-1/4} \qquad (2300 < \mathrm{Re}_{Dh,i} < 2x10^4) \tag{15}$$

$$\frac{h_i D_{h,i}}{k_i} = \frac{(f_i/2)(D_{h,i} - 10^3)\,\mathrm{Pr}_i}{1 + 12.7(f_i/2)^{1/2}(\mathrm{Pr}^{2/3} - 1)} \qquad (2300 < \mathrm{Re}_{Dh,i} < 5x10^6) \tag{16}$$

Assuming diffusion to be the dominant transport mechanism across the diffusion and catalyst layer (Bird *et al.*, 2002), the fuel and oxidant mass fluxes are given by

$$j_i = -\left[D(\rho_{out} - \rho_{in})/L\right]_i \tag{17}$$

Where, according to Newman (1991), $D = B\left\{T^{\left[8\bar{R}T/\pi M\right]^{1/2}\phi^q}\right\}$, is the Knudsen diffusion coefficient. Therefore

$$P_{i,out} = P_{i,in} - \frac{j_i R_k T_\infty L_i \theta_i}{D_i p_\infty}, \quad \text{i = 2,6; k = f,ox} \tag{18}$$

The net heat transfer rates at CV2 are $\tilde{Q}_2 = -\tilde{Q}_{12} + \tilde{Q}_{w2} + \tilde{Q}_{23} + \tilde{Q}_{2ohm}$, where $\tilde{Q}_{23} = \tilde{k}_{s,a}(1-\phi_2)\tilde{A}_s(\theta_2 - \theta_3)/[(\xi_2 + \xi_3)/2]$, where the subscript s,a indicates the solid anode side. The energy balance for the CV2 is:

$$(\theta_1 - \theta_2) + \frac{\tilde{Q}_2}{\psi_{H_2}} = 0 \tag{19}$$

The chemical reaction that occurs at the anode reaction layer (CV3) in an AMFC is,

$$H_2 + 2OH^- \rightarrow 2H_2O + 2e^- \tag{20}$$

The dimensionless enthalpy of formation is defined by $\tilde{H}_i = \dot{n}_i H_i / \left(\dot{m}_{ref} c_{p,f} T_\infty\right)$, where the subscript i refers to a substance or a control volume, H is the enthalpy of formation, kJ/kmol. The enthalpy change due to the anode reaction is given by $\Delta H_3 = \sum_{products}[\upsilon_i H_i(T_i)] - \sum_{reactants}[\upsilon_i H_i(T_i)]$ and $W_{e3} = -\Delta G_3$, where υ is the reaction stoichiometric coefficient, W_{e3} is the reversible work done by the CV3, J. The reaction Gibbs free energy change, ΔG, is a function of temperature, pressure and concentrations (Masterton and Hurley, 1997).

$$\Delta G = \Delta G^0 + \bar{R} T \ln Q \tag{21}$$

where $\bar{R}$ is the universal gas constant, 8.314 kJ/kmolK; $\Delta G^0 = \Delta H^0 + T^0 \Delta S^0$, ΔG is the molar Gibbs free energy change, kJ/kmol; ΔH is the molar enthalpy change, kJ/kmol; ΔS is the molar entropy change kJ/kmol; the superscript ^{0} indicate standard conditions (gases at 1 atm, 25°C, species in solution at 1 M), Q is the reaction quotient. In the present reaction, Eq. (18) the resulting expression for Q_3 is $Q_3 = \left\{\left[OH^-\right]^2 p_{H_2}\right\}^{-1}$, where $\left[OH^-_{(aq)}\right]^2$ is the molar concentration of the alkaline solution, (mol l^{-1}), and $p_{H_2} = p_{2,out}$, i.e. the H_2 partial pressure in atmospheres at the CV2 outlet. The dimensionless net heat transfer in CV3 is given by $\tilde{Q}_3 = -\tilde{Q}_{23} + \tilde{Q}_{w3} + \tilde{Q}_{34} + \tilde{Q}_{3ohm}$. The heat transfer rate between CV3 and CV4 (alkaline membrane) is dominated by conduction, therefore $\tilde{Q}_{34} = -(1-\phi_3)(\theta_3 - \theta_4)\tilde{A}_s 2\tilde{k}_{s,a}\tilde{k}_m / (\xi_4 \tilde{k}_{s,a} + \xi_3 \tilde{k}_m)$, where $\tilde{k}_m$ is the dimensionless thermal conductivity of the membrane (CV4). The energy balance for CV3 is

$$\tilde{Q}_3 - \Delta\tilde{H}_3 + \Delta\tilde{G}_3 = 0 \tag{22}$$

where, $(\Delta\tilde{H}_3, \Delta\tilde{G}_3) = \dot{n}_{H_2}(\Delta H_3, \Delta G_3) / \left(\dot{m}_{ref} c_{p,f} T_\infty\right)$.

The dimensionless net heat transfer in CV4 is obtained from $\tilde{Q}_4 = -\tilde{Q}_{34} + \tilde{Q}_{w4} + \tilde{Q}_{45} + \tilde{Q}_{4ohm}$ and $\tilde{Q}_{45} = -(1-\phi_5)(\theta_4 - \theta_5)\tilde{A}_s 2\tilde{k}_{s,c}\tilde{k}_m / (\xi_4 \tilde{k}_{s,c} + \xi_5 \tilde{k}_m)$. Next, the CV4 temperature is obtained from

$$\tilde{Q}_4 + \tilde{H}(\theta_5)_{OH^-} - \tilde{H}(\theta_4)_{OH^-} - \tilde{H}(\theta_3)_{H_2O} - \tilde{H}(\theta_4)_{H_2O} = 0 \tag{23}$$

In the cathode reaction layer (CV5), the following reaction occurs

$$\frac{1}{2} O_2 + 2H_2O + 2e^- \rightarrow 2OH^- \tag{24}$$

The CV5 dimensionless temperature is obtained by

$$\tilde{Q}_5 - \Delta\tilde{H}_5 + \Delta\tilde{G}_5 = 0 \tag{25}$$

where $(\Delta\tilde{H}_5, \Delta\tilde{G}_5) = \dot{n}_{O_2}(\Delta H_5, \Delta G_5) / \left(\dot{m}_{ref} c_{p,f} T_\infty\right)$.

Similarly, the dimensionless net heat transfer rate flowing in CV5 is given by $\tilde{Q}_5 = -\tilde{Q}_{45} + \tilde{Q}_{w5} + \tilde{Q}_{56} + \tilde{Q}_{5ohm}$, with $\tilde{Q}_{56} = -\tilde{k}_{s,c}(1-\phi_6)\tilde{A}_s(\theta_5 - \theta_6) / \left[(\xi_5 + \xi_6)/2\right]$.

The enthalpy change during cathode reaction is $\Delta H_5 = \sum_{products}[\upsilon_i H_i(T_i)] - \sum_{reactants}[\upsilon_i H_i(T_i)]$, while $W_{e5} = -\Delta G_5$. The CV5 reaction quotient is $Q_5 = \left[OH^-\right]^2 / p_{O_2}^{1/2}$, where $p_{O_2} = p_{6,out}$.

The dimensionless net heat transfer rate in CV6 results from $\tilde{Q}_6 = -\tilde{Q}_{56} + \tilde{Q}_{w6} + \tilde{Q}_{67} + \tilde{Q}_{6ohm}$, with $\tilde{Q}_{67} = \tilde{h}_7 \tilde{A}_s (1-\phi_6)(\phi_7 - \phi_7)$, $\tilde{h}_7 = h_7 V_T^{2/3} / \left(\dot{m}_{ref} c_{p,f}\right)$. The dimensionless temperature for CV6 is given by

$$\tilde{Q}_6 + \psi_{O_2} \frac{c_{p,ox}}{c_{p,f}} (\theta_7 - \theta_6) + \tilde{H}(\theta_5)_{H_2O} - \tilde{H}(\theta_6)_{H_2O} = 0 \tag{26}$$

The dimensionless net heat transfer rate in CV7 is $\tilde{Q}_7 = -\tilde{Q}_{67} + \tilde{Q}_{w7} + \tilde{Q}_{7ohm}$. The balances for mass and energy in the oxidant channel (CV7), the assumptions of non-mixing flow, and the assumption that the space is filled mainly with dry oxygen, yield $\dot{m}_{H_2O} = \dot{m}_{H_2O,in} = \dot{m}_{H_2O,out} = \dot{n}_{O_2} M_{H_2O}$ and

$$\tilde{Q}_7 + \psi_{ox}\frac{c_{p,ox}}{c_{p,f}}(\theta_{ox}-\theta_7) + \tilde{H}(\theta_6)_{H_2O} - \tilde{H}(\theta_7)_{H_2O} = 0 \tag{27}$$

2.2. Electrochemical model

Based on the electrical conductivities and geometry of each compartment, the electrical resistances, $\beta(\Omega)$, are given by:

$$\beta_i = \frac{\xi_i}{\tilde{A}_s V_T^{1/3}\sigma_i(1-\phi_i)}, \qquad \text{i = 1,2,6,7} \tag{28}$$

$$\beta_i = \frac{\xi_i}{\tilde{A}_s V_T^{1/3}\sigma_i\phi_i}, \qquad i\text{= 3, 4, 5, } (\phi_4 = 1) \tag{29}$$

We considered the electrical conductivities $\sigma_i = \sigma_{solution}$ for i=3,4,5. The conductivities of the diffusive layer, σ_2 and σ_6, are the carbon-phase conductivities (Kulikovsky, 2000). Finally, the conductivities of CV1 and CV7, σ_1 and σ_7, are given by the electrical conductivity of the bipolar plate material.

The appropriate figure of merit for evaluating the performance of a fuel cell is the polarization curve, i.e., the fuel cell total potential as a function of current. The dimensionless potential is defined in terms of a given reference voltage, V_{ref}, namely $\tilde{V} = V/V_{ref}$ and $\tilde{\eta} = \eta/V_{ref}$, where V is the voltage of the fuel cell, V; η is the overpotential, V; $\tilde{\eta}$ is the dimensionless overpotential, and $\tilde{V}$ is the dimensionless voltage of the fuel cell. The dimensionless actual potential $\tilde{V}_i$ is an accumulated result of dimensionless irreversible anode electrical potential $\tilde{V}_{i,a}$, dimensionless irreversible cathode electrical potential $\tilde{V}_{i,c}$, and the dimensionless ohmic loss $(\tilde{\eta}_{ohm})$ in the space from CV1 to CV7, i.e.,

$$\tilde{V}_i = \tilde{V}_{i,a} + \tilde{V}_{i,c} - \tilde{\eta}_{ohm} \tag{30}$$

The ohmic loss $\tilde{\eta}_{ohm}$ is estimated by

$$\tilde{\eta}_{ohm} = \frac{I}{V_{ref}}\sum_{i=1}^{7}\beta_i \tag{31}$$

The reversible electrical potential at the anode is given by the Nernst equation,

$$V_{e,a} = V_{e,a}^o - \frac{\bar{R}T_3}{nF}\ln Q_3 \tag{32}$$

where $V_{e,a} = \Delta G_3/(-nF)$ and $V_{e,a}^o = \Delta G_3^o/(-nF)$. At the anode there are two mechanisms for potential losses; (i) charge transfer, and (ii) mass diffusion. The potential loss at the anode (η_a) due to charge transfer is obtained implicitly from the Butler-Volmer equation for a given current I (Gurau *et al.*,2000)

$$\frac{I}{A_{3,wet}} = i_{o,a}\left\{\exp\left[\frac{(1-\alpha_a)\eta_a F}{\bar{R}T_3}\right] - \exp\left[-\frac{\alpha_a\eta_a F}{\bar{R}T_3}\right]\right\} \tag{33}$$

Where α_a is the anode charge transfer coefficient and $i_{o,a}$ is the anode exchange current density.

The potential loss due to mass diffusion is

$$\eta_{d,a} = \frac{\bar{R}T_3}{nF}\ln\left(1 - \frac{I}{A_{3,wet}i_{Lim,a}}\right) \tag{34}$$

Where,

$$i_{\lim,a} = \frac{p_f D_2 nF}{M_{H_2} L_2 R_f \theta_2 T_\infty} \tag{35}$$

The resulting electrical potential at the anode is $\tilde{V}_{i,a} = \tilde{V}_{e,a} - \tilde{\eta}_a - \left|\tilde{\eta}_{d,a}\right|$.

The methodology in estimating the anode potential is valid in building the cathode potential correlations. Similarly, the actual cathode potential is $\tilde{V}_{i,c} = \tilde{V}_{e,c} - \tilde{\eta}_c - \left|\tilde{\eta}_{d,c}\right|$ and the reversible electrical cathode potential is $V_{e,c} = V^o_{e,c} - \left(\bar{R}T_5/nF\right)\ln Q_5$, where $V^o_{e,c} = \Delta G^o_5/(-nF)$. The Butler-Volmer equation for calculating the cathode side overpotential η_c is $I/A_{5,wet} = i_{o,c}\left[\exp\left((1-\alpha_c)\eta_c F/\left(\bar{R}T_5\right)\right) - \exp\left(\alpha_c \eta_c F/\left(\bar{R}T_5\right)\right)\right]$ where α_c is the cathode charge transfer coefficient, and $i_{o,c}$ is the cathode exchange current density. The cathode mass diffusion depleting overpotential is $\eta_{d,c} = \bar{R}T_5/(nF)\ln\left(1 - I/\left(A_{5,wet} i_{Lim,c}\right)\right)$, and the cathode limiting current density is $i_{\lim,c} = 2\, p_{ox} D_6 nF/\left(M_{O_2} L_6 R_{ox} \theta_6 T_\infty\right)$.

2.3. Fuel cell net power output

The pumping power $\tilde{W}_p$ is required to supply the fuel cell with fuel and oxidant. Therefore the total net power (available for utilization) of the fuel cell is

$$\tilde{W}_{net} = \tilde{W} - \tilde{W}_p \tag{36}$$

where $\tilde{W} = \tilde{V}_i \tilde{I}$ is the total fuel cell electrical power output , and

$$\tilde{W}_p = \psi_f S_f \frac{\theta_i}{Pi}\Delta P_1 + \psi_{ox} S_{ox} \frac{\theta_7}{P_7}\Delta P_7 \tag{37}$$

$$S_f = \frac{m_{ref} T_\infty R_i}{V_{ref} I_{ref}}, \quad i = f,ox \tag{38}$$

3 NUMERICAL RESULTS OF AMFC MODEL

The single AMFC net power output, defined by Eq. (36), depends on the internal structure and the external shape of the fuel cell. The mathematical model allows the computation of the total net power of the fuel cell, which is possible to be done as soon as the physical values and a set of geometric internal and external parameters are known. In the case of the present study, such set is given by Tab. 1.

The numerical simulation of the single AMFC is performed by solving Eqs. (7), (18), (19), (22), (23), (25), (26) and (27) which form a system of nine algebraic equations. The unknowns are θ_i and P_i, i.e., the temperatures in the seven control volumes, and the gas pressures in CV2 and CV6. Once the temperatures and pressures are known, the electrical potentials and power are calculated for any assumed current level. Pressures are related to temperatures via Eq. (18). The system reduces to seven nonlinear algebraic equations, in which the unknowns are the temperatures of the seven control volumes. This system was solved with a Fortran code, using a quasi-Newton method (Kincaid and Cheney, 1991), where a tolerance for the norm of the residual vector less or equal to 10^{-6} was considered to obtain a converged solution.

In the numerical simulations, the cells electrical and net power were calculated by starting from open circuit $\left(\tilde{I} = 0\right)$, and proceeding with increments of $\left(\Delta\tilde{I} = 5\right)$ until the net power is zero or the limiting current level is reached. The reference case for the simulation is a alkaline fuel with the following internal and external configuration $\xi_1/\xi_x = \xi_7/\xi_x = 0.38$, $\xi_2/\xi_x = \xi_6/\xi_x = 0.111$, $\xi_3/\xi_x = \xi_5/\xi_x = 0.0025$, $\xi_4/\xi_x = 0.013$.

Because we assume that no losses result from species crossover from one electrode through the electrolyte and from internal currents, the actual open circuit voltage is equal to the reversible cell potential (ideal case).

Table 1. Physical properties used as reference case in the numerical solution.

$B = 0.156$	$q = 1.5$
$c_{p,f} = 14.95$ kJ kg^{-1} K^{-1}	$R_f = 4.157$ kJ kg^{-1} K^{-1}
$c_{p,ox} = 0.91875$ kJ kg^{-1} K^{-1}	$R_{ox} = 0.2598$ kJ kg^{-1} K^{-1}
$c_{v,f} = 10.8$ kJ kg^{-1} K^{-1}	T_f, T_{ox}, $T_\infty = 298.15$ K
$c_{v,ox} = 0.659375$kJ kg^{-1} K^{-1}	$U_{wi} = 50$ W m^{-2} K^{-1}, i = 1 to 7
$(i_{0,a}, i_{0,c}) = (0.01, 0.005)$ A m^{-2}	$V_{ref} = 1$ V
$I_{ref} = 1$ A	$V_T = 7\times10^{-5}$ m^3
$k_f = 0.1805$ W m^{-1} K^{-1}	$\alpha_a, \alpha_c = 0.5$
$k_{ox} = 0.0266$ W m^{-1} K^{-1}	$\zeta_1, \zeta_7 = 2$
$k_p = 0.12$ W m^{-1} K^{-1}	$\mu_1 = 10^{-5}$ Pa.s
$K_2, K_6 = 4 \times 10^{-10}$ m^2	$\mu_7 = 2.4\times10^{-5}$ Pa.s
$K_3, K_5 = 4 \times 10^{-12}$ m^2	$\phi_2, \phi_6 = 0.0085$
$\dot{m}_{ref} = 10^{-5}$ kg s^{-1}	$\phi_3, \phi_5 = 0.1802$
$p_f = 0.1$ MPa	
$p_{ox}, p_\infty = 0.12$ MPa	

At low currents, the potential drop is due to activation losses, low catalysis; in the next region the ohmic losses are present (due to electrical resistance of the components of the fuel cell) and at high currents the concentration losses are dominant. This behavior is shown in the Fig. 3.

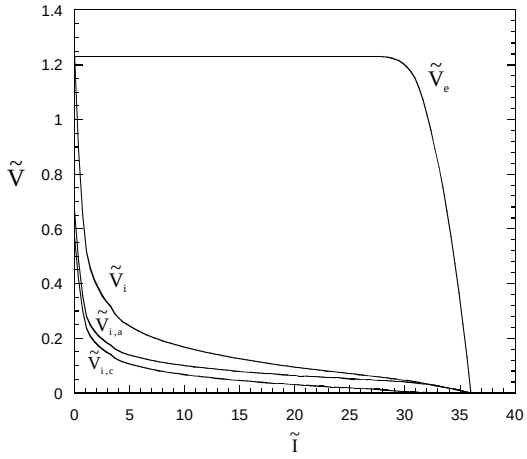

Figure 3. Polarization curves of AMFC. $\tilde{V}_e$ is the dimensionless reversible potential, $\tilde{V}_{i,a}$, $\tilde{V}_{i,c}$ is the dimensionless reversible potential at the anode and cathode, respectively and $\tilde{V}_i$ is the dimensionless irreversible potential of the fuel cell.

The total potential is the sum of the potential generated at the cathode and anode minus all the losses evaluated (activation. Ohmic and concentration losses). Since the Gibbs free energy decreases as the temperature increases, the reversible potential decreases as well, Eq. (32). From Eq. (18) we can see that the pressure of the reactants eventually decreases to zero as the current increases, since the consumption of oxygen and hydrogen increases. This is the limit case when the potential of the electrode reaches zero. The simulation was conducted until the point where we reach the concentration polarization region where the irreversible voltage approaches to zero, see Fig. 4. The current where we obtained the maximum power was at $\tilde{I} = 16$.

As it is shown in the Fig. 5, the temperature of the fuel cell increases as the current increases, since more heat is being generated in the electrochemical reactions and by the Joule effect. This profile demonstrates that the temperature in am AMFC is not constant as sometimes is considered. This model takes the temperature distribution into account when evaluates the polarization curve and the total power output, since the Eq. (32) tells us that the voltage is a function of temperature.

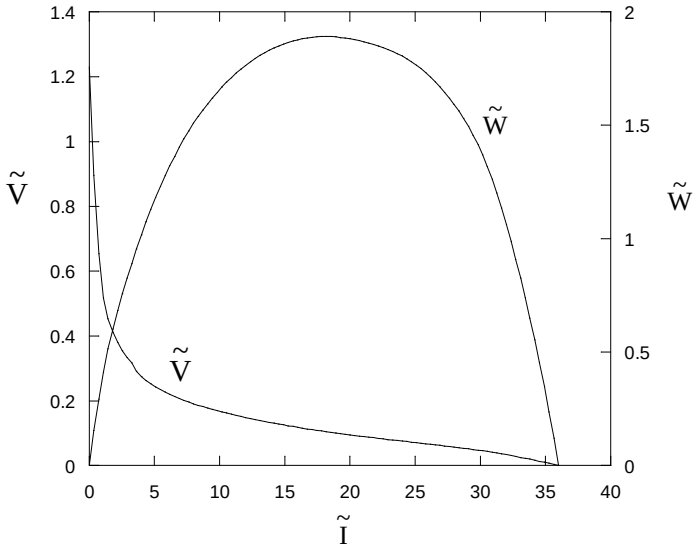

Figure 4. Total cell output voltage and power simulated numerically, $\tilde{V}$ is the dimensionless total output voltage and $\tilde{W}$ is the dimensionless total output work.

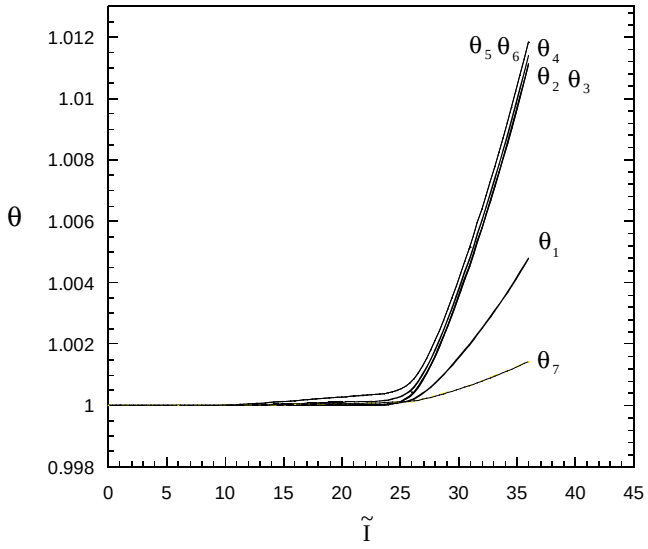

Figure 5. Temperature versus current for the reference case of an AMFC.

For the current interval evaluated, the temperature's variation was not significant. Although it will have more influence when a scale-up or a AMFC stack is used.

4 CONCLUSION

In this paper we constructed a model for fluid flow, mass and heat transfer in a unit AMFC which takes into account spatial temperature and pressure gradients. The model shows good results in predicting the voltage and power output, considering the pressure drop in the channel of gas. The results also show that even in a unit fuel cell at low currents, there is a gradient of temperature dependent of space and current. The model was base on fixed anode and cathode exchange current densities, which depend on catalyst type and morphology, temperature and pressure. These parameters increase with temperature, however the increase of temperature also increase the activation losses, (O'Hayre, *et al.*, 2009). The present model can be used as a tool for optimization where the electrical power can be maximized, considering temperature gradient and the pressure drop in the channels (Fig. 1).

5 ACKNOWLEDGEMENTS

Acknowledgments for the Conselho Nacional de Desenvolvimento Científico e Tecnológico - CNPq for the sponsorship of this research. Also, acknowledgments for the Mechanical Engineer Post Graduations Program (PGMEC) of the Universidade Federal do Paraná and Center for Advanced Power Systems (CAPS) of Florida State University.

6 REFERENCES

Bejan, A., 1995, "Convection Heat Transfer", second ed., Wiley, 988 New York.
Bird, R. B., Stewart, W. E., Lightfoot ,E. N., 2002, "Transport Phenomena", second ed., Wiley, New York.
Gurau ,V., Barbir, F., Liu, H., 2000, "An analitical solution of a half-cell model for PEM fuel cells", J. Electrochem. Soc. No. 147, pp 2468-2477.
Kincaid, D., Cheney, W., 1991, "Numerical Analysis Mathematics of Scientific Computing", first ed., Wadsworth, Belmont, CA.
Kulikovsky, A. A., Divisek ,J., Kornyshev, A. A., 2000, "Two-dimensional simulation of direct methanol fuel cells –a new (embedded) type of current collector", J. Electrochem. Soc. No. 147, pp. 953-959.
Masterton, W. L., Hurley, C. N., 1997, "Chemistry Principles & Reactions", third ed., Saunders College Publishing, Orlando, FL.
Newman, J. S., 1991, "Electrochemical Systems", second ed., Prentice Hall, Englewood Cliffs, NJ, pp. 255, 299, 461.
O'Hayre, R., Cha, S., Colella, W., Prinz, F. B., 2009, "Fuel Cell Fundamentals" Second ed.,New Jersey.
Shah, R. K., and London, A. L., " Laminar Flow Forced Convection in Ducts, Supplement 1 to Advances in Heat Transfer", Academic Press, New York, 1978.
Vargas, J. V. C. ; Gardolinski, J. E. F. C.; Ordonez, J. C. Hovsapian, R. ALKALINE MEMBRANE FUEL CELL. Patent, USPTO application number 61/067,404 – 2008.

7 RESPONSIBILITY NOTICE

The authors are the only responsible for the printed material included in this paper.